



Full-scale field test of a model predictive control system for a 3 MW wind turbine

Sebastian Dickler¹ · Thorben Wintermeyer-Kallen¹ · János Zierath² · Reik Bockhahn² · Dirk Machost² · Thomas Konrad¹ · Dirk Abel¹

Received: 2 December 2020 / Accepted: 5 March 2021 / Published online: 9 April 2021
© The Author(s) 2021

Abstract

Model predictive control (MPC) is a strong candidate for modern wind turbine control. While the design of model predictive wind turbine controllers in simulations has been extensively investigated in academic studies, the application of these controllers to real wind turbines reveals open research challenges. In this work, we focus on the validation of a linear time-variant MPC system for a 3 MW wind turbine in a full-scale field test. First, the study proves the MPC's capability to control the real wind turbine in the partial load region. Compared to the turbine's baseline PID controller, the MPC system offers similar results for the electrical power output and for the occurring mechanical loads. Second, the study validates a previously proposed, simulation-based rapid control prototyping process for a systematic MPC development. The systematic development process allows to completely design and parameterize the MPC system in a simulative environment independent of the real wind turbine. Through the rapid control prototyping process, the MPC commissioning in the wind turbine's programmable logic controller can be realized within a few hours without any modifications required in the field. Thus, this study establishes the proof of concept for a linear time-variant MPC system for a 3 MW wind turbine in a full-scale field test and bridges the gap between the control design and field testing of MPC systems for wind turbines in the multi-megawatt range.

✉ Sebastian Dickler
sebastian.dickler@rwth-aachen.de

¹ Institute of Automatic Control, RWTH Aachen University,
Campus-Boulevard 30, 52074 Aachen, Germany

² W2E Wind to Energy GmbH,
Grubenstraße 44, 18055 Rostock, Germany

Feldtest eines Modellprädiktiven Regelungssystems an einer realen 3-MW-Windenergieanlage

Zusammenfassung

Die Modellprädiktive Regelung (engl. model predictive control, MPC) bietet einen vielversprechenden Ansatz für die moderne Windenergieanlagen-Regelung. Während der Entwurf von MPC für Windenergieanlagen umfassend in simulativen Studien untersucht wurde, weist die Umsetzung dieser Regelungen für reale Windenergieanlagen weiterhin offene Forschungsfragen auf. Die vorliegende Studie konzentriert sich auf die Validierung eines linearen zeitvarianten MPC-Systems für eine 3-MW-Windenergieanlage in einem Feldtest mit der realen Anlage. Die Arbeit weist dabei einerseits die Fähigkeit der Modellprädiktiven Regelung nach, die reale Windenergieanlage im Teillastbereich zu regeln: Das MPC-System liefert Ergebnisse für die elektrische Leistung sowie für die auftretenden mechanischen Lasten, die vergleichbar sind mit denen der Basis-PID-Regelung der Windenergieanlage. Andererseits validiert die Studie einen zuvor vorgeschlagenen, simulationsgestützten Rapid-Control-Prototyping-Prozess zur systematischen MPC-Entwicklung. Der systematische Entwicklungsprozess ermöglicht es, das MPC-System vollständig in einer Simulationsumgebung zu entwerfen und zu parametrieren – unabhängig von der realen Windenergieanlage. Durch den Rapid-Control-Prototyping-Prozess kann die Inbetriebnahme des MPC-Systems in der speicherprogrammierbaren Steuerung der realen Windenergieanlage innerhalb weniger Stunden realisiert werden, ohne dass dabei Anpassungen erforderlich sind. Damit erbringt die vorliegende Studie den Proof-of-Concept für das lineare zeitvariante MPC-System für die 3-MW-Windenergieanlage in einem Feldtest mit der realen Anlage und schließt die Lücke zwischen dem Regelungsentwurf und dem Feldtest von MPC-Systemen für Windenergieanlagen im Multi-Megawatt-Bereich.

1 Introduction

Efficient wind turbine operation takes an essential role in wind energy technology as part of the energy transition. Applying advanced control strategies to real wind turbines (WTs) is challenging but at the same time vital for the success of the WT technology [1].

In this work, we present experimental results of a full-scale field test conducted with a model predictive control (MPC) system in July 2020 in a 3 MW WT (type “W2E-120/3.0fc”) designed and built by *W2E Wind to Energy GmbH* [2]. With this work, we verify the proposed development process from [3] and validate the functional and structural integration of the MPC system into the existing automation system. Thus, this study bridges the existing gap between the MPC’s design and its field testing.

Our companion paper [4] presents the real-time implementation of the linear time-variant MPC algorithm evaluated in the field test in detail. In the following, we focus on the test setup and the analysis of the field test results.

1.1 Theory and research

MPC is a promising approach for the control of modern WTs: It benefits from its abilities to handle multi-variable control problems and to consider process constraints explicitly for calculating optimal values for the manipulated variables.

The application of MPC algorithms in real WTs requires comprehensive testing throughout the entire development process. While the simulative design of MPCs for WTs has been extensively investigated in academic studies [5], the

application of these controllers to real WTs reveals open research challenges throughout the hardware-oriented development process (see [1, 6, 7]).

Regarding full-scale field testing, [8] evaluated trailing edge flaps in a full-scale WT of the type “Vestas V27” (nominal power of 225 kW) with active load reduction using a frequency-weighted MPC. To the authors’ best knowledge, field test results with a full-scale WT in the multi-megawatt range using MPC are not published so far.

Although the implementation and testing in industrial hardware are vital prior to the evaluation of a new (model predictive) control system in field tests, only very few studies addressed these development steps in hardware-in-the-loop tests. However, studies, such as [6] and [9], validated MPC algorithms for WTs in system simulations and verified the implementation’s real-time capability in a standard computer hardware. Furthermore, [10] conducted wind tunnel tests with a small-scale wind turbine using an MPC algorithm also executed in standard computer hardware. Moreover, [11] focuses on the computational performance of a nonlinear MPC and a moving horizon estimator for airborne wind energy systems using automatic code generation for the experimental validation in an industrial PC. Among these studies, we have already investigated the hardware-in-the-loop testing of MPC systems for WTs in [12].

In [3], we propose a comprehensive development environment and a systematic development process for designing and testing MPC systems for WTs in system simulations, software-in-the-loop (SiL) and hardware-in-the-loop (HiL) tests. In particular, [3] demonstrates control operation over the entire operating range in SiL tests and verified

the MPC’s real-time capability in the WT’s programmable logic controller (PLC) in HiL tests.

1.2 Research objectives

First, this study aims to provide the proof of concept for the capability of the MPC system to control the real WT in the field. Second, this study seeks to validate the continuous toolchain and holistic development environment presented in [3], which enables a systematic MPC development for WTs in order to reduce the application effort in the field.

To this end, we compare the experimental MPC results with the experimental results of the WT’s baseline controller as well as with the simulative MPC results in order to identify open issues for the MPC design and potential improvements for the systematic development process from [3].

The paper is organized as follows. Sect. 2 presents the MPC algorithm as well as the field test setup with a brief description of the WT and its automation system. Sect. 3 presents, analyzes and discusses the field test results and identifies potential improvements for the MPC design and the systematic MPC development process. Finally, Sect. 4 concludes the overall findings and identifies avenues for future research.

2 Methods

In this section, we introduce the MPC algorithm to be tested in the field and specify the test setup of the real WT and its automation system.

2.1 MPC for the 3 MW wind turbine

Our companion paper [4] presents the real-time implementation of the linear time-variant MPC algorithm with weight-scheduling evaluated in the field test in detail. This section recapitulates the MPC formulation and underlines the algorithm characteristics relevant for the field test.

The control system has the following control objectives:

1. maximizing the electrical power output,
2. mitigating dynamic mechanical loads, and
3. maintaining operating limits.

The MPC system comprises an MPC algorithm and an extended Kalman filter (the state observer has already been described in detail in [13]). The MPC algorithm solves the online optimization problem

$$\Delta \mathbf{u}_{\text{opt}}(\cdot|k) = \arg \min_{\Delta \mathbf{u}(\cdot|k)} J(\Delta \mathbf{u}(\cdot|k)) \tag{1}$$

subject to constraints in order to maintain limits for the manipulated, state and controlled variables. The MPC recursively calculates the optimal trajectory of the manipulated variables $\Delta \mathbf{u}_{\text{opt}}(\cdot|k)$ by minimizing the quadratic cost function

$$J = \|\mathbf{y}(\cdot|k) - \mathbf{y}_{\text{ref}}(\cdot|k)\|_{\mathbf{Q}(\mathbf{y}(k))}^2 + \lambda \left(\|\Delta \mathbf{u}(\cdot|k)\|_{\mathbf{R}_{\Delta \mathbf{u}}(\mathbf{y}(k))}^2 + \|\mathbf{u}(\cdot|k)\|_{\mathbf{R}_{\mathbf{u}}(\mathbf{y}(k))}^2 \right) \tag{2}$$

with the variable weighting matrices \mathbf{Q} , $\mathbf{R}_{\Delta \mathbf{u}}$ and $\mathbf{R}_{\mathbf{u}}$ (referred to as weight-scheduling in [4]). The cost function penalizes the deviations between the controlled variables \mathbf{y} and their references \mathbf{y}_{ref} (for reference tracking) as well as the manipulated variables \mathbf{u} and their changes $\Delta \mathbf{u}$. The MPC has a sampling time of $\Delta T = 100$ ms and prediction and control horizons of $H_p = 5$ s and $H_u = 1$ s, respectively. We use the software qpOASES [14]—which uses an active set strategy—to solve the quadratic programming problem online.

We consider the wind speed v as disturbance variable and use the collective pitch angle rate $\dot{\vartheta}$ and the generator torque τ_{gen} as manipulated variables \mathbf{u} . We choose the generator speed ω_{gen} and the electrical (active) power p_{el} as controlled variables in order to maximize the electrical power output (objective 1). According to control objective 2, we want to mitigate the dynamic mechanical loads in fore-aft direction and choose the tower top acceleration \ddot{x}_t as controlled variable representing these loads. We use the pitch angle ϑ as additional controlled variable in order to provide a pitch reference in the partial load region. Moreover, the MPC enables an explicit consideration of constraints (e.g. $\dot{\vartheta}$ and p_{el}), which ensure maintaining the process variables within their operating limits (objective 3).

The vectors of the manipulated and controlled variables are defined by

$$\mathbf{u} = (\dot{\vartheta} \quad \tau_{\text{gen}})^T, \tag{3}$$

$$\mathbf{y} = (\omega_{\text{gen}} \quad p_{\text{el}} \quad \ddot{x}_t \quad \vartheta)^T. \tag{4}$$

The applied reduced-order prediction model sufficiently represents the turbine dynamics for control purposes and yet meets the real-time requirements. The linearized, discrete time state space model used for predicting the WT’s dynamic behavior is described in detail in [4]. We define the state vector as

$$\mathbf{x} = (\omega_{\text{rot}} \omega_{\text{hub}} \omega_{\text{gen}} \varphi_{\text{rh}} \varphi_{\text{hg}} \ x_t \ \dot{x}_t \ \varphi_b \ \dot{\varphi}_b \ \vartheta \ v_{\text{eff}})^T. \tag{5}$$

The rotor, hub and generator speeds (ω_{rot} , ω_{hub} and ω_{gen}) as well as the angular differences between the rotor, hub and generator positions (φ_{rh} and φ_{hg}) define the WT’s drivetrain dynamics. The tower top position and velocity, x_t and \dot{x}_t , and the collective blade deflection and velocity, φ_b and

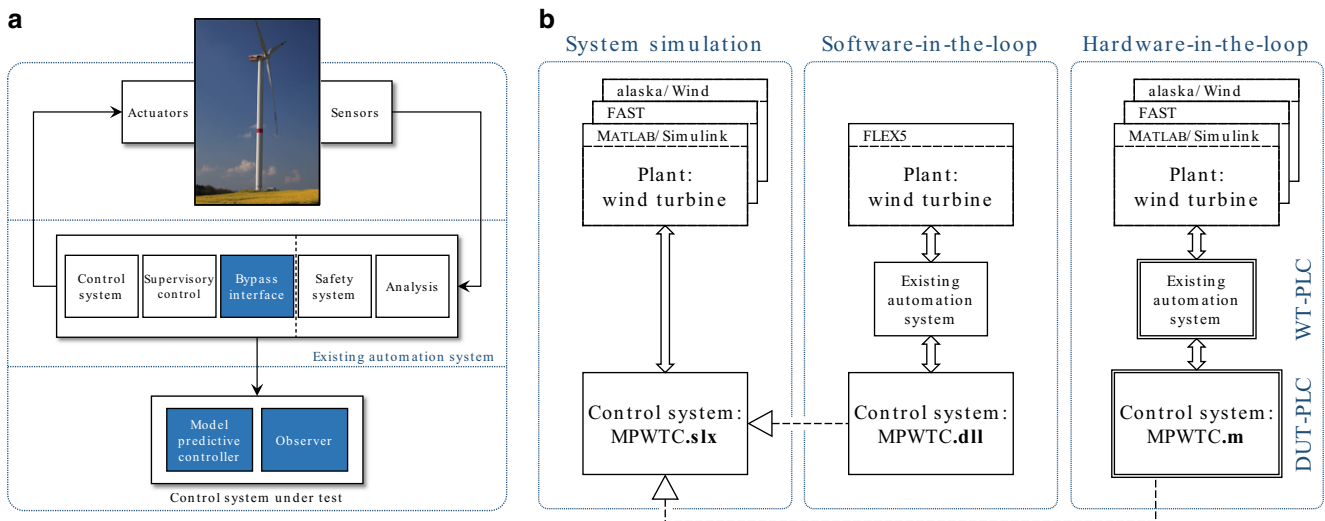


Fig. 1 a Closed loop structure of the WT’s automation system; the plant (upper image) shows the prototype of W2E’s 3 MW WT “W2E-120/3.0fc” in Rostock, Germany. b Testing stages “system simulation”, “software-in-the-loop” test and “hardware-in-the-loop” test [3]

ϕ_b , define the tower and blade dynamics. In this formulation, the pitch angle ϑ and the rotor-effective wind speed v_{eff} are additionally included in the state vector. The wind speed immediately affects the rotor speed, tower top and collective blade velocity and indirectly influences the other states due to the coupled differential equations of the system.

The weight-scheduling scheme for MPC introduced in [4] enables WT operation in the partial as well as in the full load region. Thus, the MPC algorithm provides a convex formulation of the optimization problem—which can be solved online by using the qpOASES solver—and offers the capability to adapt to the operating points over the entire operating range. For the operation in the partial as well as in the full load region, we provide reference values y_{ref} for the controlled variables y that depend on the current wind speed (estimated by the extended Kalman filter).

2.2 Field test setup

In the following, we briefly describe the WT, the WT’s automation system as well as the toolchain between the engineering PC and the WT’s PLC.

Specifications of the 3 MW WT We conducted the field test with the W2E’s horizontal axis WT “W2E-120/3.0fc” (see Fig. 1a, [2]). The variable-speed WT with medium-speed full power converter offers a rated power of 3 MW, a tower top height of 100 m and a rotor diameter of 120 m. The WT has a rated rotor speed of 12.1 rpm, and cut-in, rated and cut-out wind speeds of 3.0, 12.5 and 25.0 m/s, respectively. The mechanical and electrical WT’s components as well as their technical specifications were already described in

detail in [2]. Table 1 shows the WT’s natural frequencies relevant for the field test.

WT’s automation system We consider a software and hardware structure of the WT’s automation system as shown in Fig. 1a. We distinguish between the existing automation system and the control system under test (MPC system). The structure of the automation system corresponds to the HiL setup in [3] (see Fig. 1b). We use two separated PLCs to execute the existing automation system and the MPC system, respectively. For the field test, we use the PLC modules “MC210” and “MH230” from *Bachmann electronic GmbH*.

The existing automation system (with the baseline control system and the supervisory control; see Fig. 1a) is executed in the MC210 PLC module (hereinafter referred to as WT-PLC; see middle layer of the HiL setup in Fig. 1b). The MPC system is executed in the MH230 PLC module (hereinafter referred to as DUT-PLC (device under test PLC); see bottom layer of the HiL setup in Fig. 1b). The WT-PLC and the DUT-PLC communicate via Ethernet. The WT-PLC as well as the existing automation system correspond to the standard setup used in the WT type “W2E-120/3.0fc”.

Table 1 Natural frequencies (NFs) of W2E’s 3 MW WT “W2E-120/3.0fc”

Name	Value (Hz)	Label
Tower (fore-aft) 1st NF	0.27	f_1
Blade (flapwise) 1st NF	0.65	f_2
Blade (edgewise) 1st NF	0.92	f_3
Blade (flapwise) 2nd NF	1.70	f_4
Blade (edgewise) 2nd NF	2.65	f_5
Drivetrain 1st NF	3.50	f_6

The software modules are depicted in Fig. 1a. The DUT-PLC executes the MPC software modules. We expand the existing automation system with the “bypass interface”, which integrates the MPC system in the WT’s automation system and enables exchanging the measured and manipulated variables. The bypass interface also decides which control system is active during the field test based on the current operating point.

The two stages of the hardware and software structure (compare Fig. 1) offer the following advantages:

1. use of identical hardware and software interfaces in the HiL test and in the field test,
2. ensuring safe operation through the physical separation of the PLCs.

The separation of the WT-PLC and the DUT-PLC enables the use of the existing WT’s automation system by only implementing the bypass interface without modifying the software modules of the existing automation system. Thus, this setup can be used for any WT’s automation system and is not limited to this specific field test or WT type. In particular, with this test setup, any PLC module can be used to execute the MPC system under test.

Toolchain engineering PC—DUT-PLC We use a continuous toolchain from the Matlab/Simulink environment in the engineering PC to the DUT-PLC in the real WT. The toolchain provides automatic code generation of the MPC code customized for the target PLC hardware; we use Bachmann’s software “M-Target for Simulink”. With the continuous toolchain, we ensure conducting prior SiL and HiL and subsequently field tests in an integrated environment using the same model instances throughout the entire development process. In [3], the toolchain and the development environment for preparing MPC algorithms for field tests are described in detail.

3 Field test of the MPC system

In this section, we evaluate the commissioning of the MPC system and present the experimental results of the field test conducted in July 2020. We analyze the collected data regarding the MPC performance and we compare the experimental results of the MPC system and the WT’s baseline controller (BC) in order to identify differences between both control systems. The BC is a state-of-the-art single-input single-output PID controller, that is currently used in the real WT [15]. Moreover, we compare the experimental MPC results with simulative MPC results from SiL tests to enhance the assumptions for the simulation models and the model-based development process. For a detailed analysis

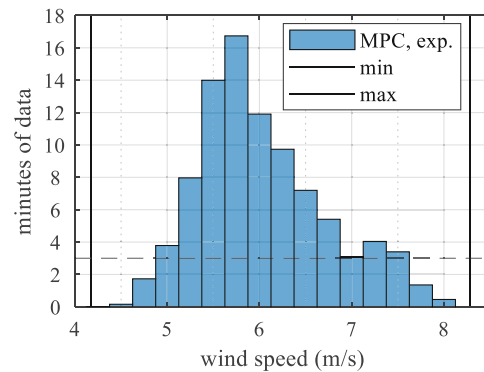


Fig. 2 Distribution of experimental data collected with the MPC system during the field test. Estimated wind speed (minimal and maximal values of 4.2 and 8.3 m/s). Horizontal line indicates threshold of 3 min and marks data with enough data points for further statistical analysis

of the load reduction with a simulative SiL test we refer to [4].

The field test aims to evaluate the MPC algorithm in the real WT for the first time. Moreover, the field test serves as a proof of concept for the continuous toolchain and the comprehensive test environment from [3]. In the field test, we collected approximately 90 min (with a sampling time of 10 ms) of experimental data with the MPC system activated. In the following, we use the data to analyze the MPC performance and identify open issues and potential improvements for the MPC algorithm as well as for the test environment.

Fig. 2 presents the distribution of the experimental data collected during the field test with the MPC system activated and shows wind conditions in the partial load region with wind speeds between 4.2 and 8.3 m/s (estimated by the extended Kalman filter). The threshold of 3 min marks the experimental data with enough data points for a statistical analysis.

3.1 Evaluation of the MPC commissioning

The systematic development process from [3]—with comprehensive system simulations, SiL and HiL tests—aims to reduce the application complexity arising during the commissioning of an MPC system in the real WT. The holistic design and testing approach strives for shifting most of the application effort in the simulative development environment.

In the field test, we were able to conduct the commissioning of the MPC system within one day in a few hours without any modifications required during the commissioning. The MPC system took over the control operation in the partial load region as expected in the preparatory simulative SiL and HiL tests. Thus, the systematic testing process has made it possible to do the parameterization of the MPC system entirely in the simulative environment.

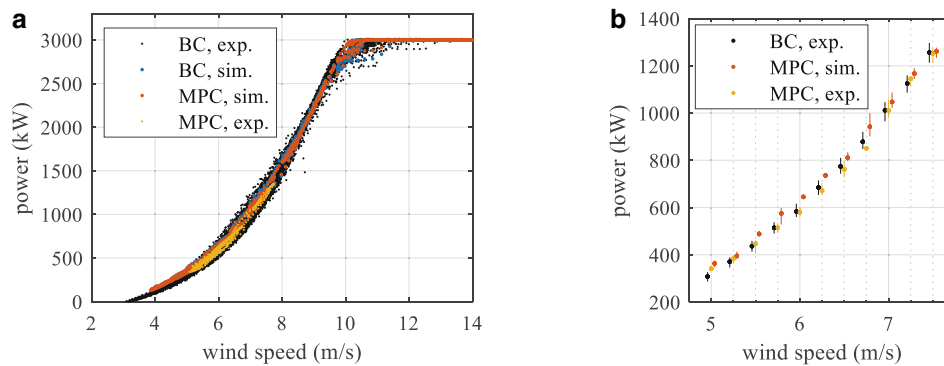


Fig. 3 Power curves of the BC and the MPC system for the experimental field test data and the simulative SiL test data: **a** Scatter plot of the generated electrical power over the estimated wind speed, and **b** extract for the wind speeds 5.0–7.5 m/s (without “BC, sim.”) for a statistic analysis of the MPC performance; with median values (*dots*) and 1st and 3rd quartiles (*vertical lines*)

3.2 Analysis of the electrical power

The maximization of the power output is the first control objective of the MPC system. To this end, we analyze the generated electrical power. First, we compare the experimental field test results of the MPC system and the BC in order to analyze the performance of the MPC controlling the real WT. The experimental field test results of the MPC system and the BC were collected during the field test in July 2020 under the same conditions. Second, we compare the MPC results of the experimental field test data with the simulative SiL test data in order to analyze the validity of the simulative test environment.

Fig. 3 provides power curves of the BC and the MPC system for the experimental field test data and the simulative SiL test data. While Fig. 3a gives an overview of the collected data, we use Fig. 3b for a detailed analysis of the MPC performance.

Fig. 3a shows a scatter plot of the generated electrical power over the estimated wind speed for the data of the BC and the MPC system. The generated power was measured by the power electronics. Since the anemometer only delivers a defective wind speed measurement in a certain measurement point behind the rotor, we use the wind speed estimated by the extended Kalman filter for the calculation of the power curve. The scatter plot uses moving average values of the generated power and the wind speed with 1-minute windows for calculating the average values in a 6-seconds sampling interval. The 6-seconds sampling is useful due to the limited number of data points.

Fig. 3b shows extracts of the power curves for the wind speeds of 5.0–7.5 m/s based on the data from Fig. 3a and depicts—corresponding to a box plot representation—the median values (*dots*) and the 1st and 3rd quartiles (*vertical lines*). In general, the median values of the experimental MPC results show a good correlation with the experimental BC results as well as with the simulative MPC results. The median values of the experimental MPC and BC results in-

dicate slight improvements using the MPC for wind speeds of 5.0–5.5 and 7.25 m/s and slight impairments for wind speeds of 6.25–6.75 m/s. The interquartile ranges (difference between the 3rd and the 1st quartile) indicate a slight improvement by the MPC system for the reference tracking by reducing the mean value of the interquartile ranges from approximately 63 kW for the BC to 48 kW for the MPC system.

In Fig. 3b, the comparison of the median values of the simulative and experimental MPC results indicates higher power outputs between 5.0–7.5 m/s for the simulative MPC results. Since the scatter plot in Fig. 3a also indicates higher power outputs for the simulative BC results compared to the experimental BC results, we assume that model uncertainties of the WT plant model cause the divergence between the simulative and experimental results.

Due to the limited number of data samples, the calculation of the annual power production would not provide reliable statements for the annual energy production. Hence, we omit this analysis for the experimental data.

3.3 Analysis of the mechanical loads

The mitigation of the dynamic mechanical loads is the second control objective of the MPC system. A direct analysis of the mechanical loads arising in the field test demands a WT setup with sensors that directly measure or reliably estimate the mechanical loads or the mechanical stress. Since the WT is equipped with standard sensors (neither load sensors nor strain gauges), we can only use these standard measurements for an indirect analysis of the mechanical load situation of the WT. To this end, we use the measurement of the tower top acceleration as indicator for loads arising due to oscillations of the fore-aft movement of the tower, and we use measurements of the rotational speeds as indicator for loads arising due to oscillations in the drivetrain.

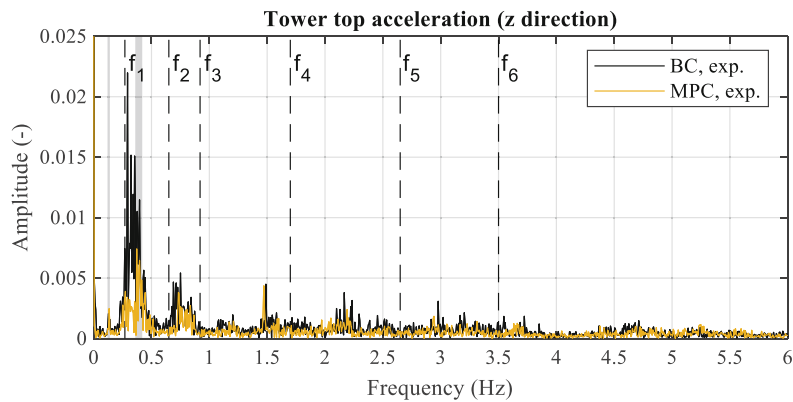


Fig. 4 FFT of the measured tower top acceleration in fore-aft (z-)direction of the experimental field test data. The plot shows the natural frequencies f_1 – f_6 from Table 1 as well as the 1P- and 3P-frequencies (grey boxes; approx. at 0.13 and 0.39 Hz, respectively). The WT operate in the partial load region. The FFT plots are based on signals with a length of 300 s (sampling time of 10 ms) and rotational speeds between 7.3 and 8.3 rpm (referred to the low speed shaft) for both control systems

Tower top acceleration We use an accelerometer inside the nacelle in order to measure the tower top acceleration in fore-aft direction.

Fig. 4 shows an FFT plot for the tower top acceleration in fore-aft direction for both the BC and the MPC system of the experimental field test data. Fig. 4 also depicts the WT's natural frequencies f_1 – f_6 (see Table 1) as well as the 1P- and 3P-frequencies in the grey boxes at approximately 0.13 and 0.39 Hz, respectively. In the MPC system, the tower top acceleration is a controlled variable. The BC system provides no active tower damping.

The FFT amplitudes for both control systems indicate gain amplifications for the frequencies f_1 , f_2 , f_4 , f_6 (representing the natural frequencies of the tower, the blades (flapwise, 1st and 2nd) and the drivetrain). In addition, gain amplifications can be found at the 1P- and 3P-frequencies. Further gain amplifications can be found at frequencies of approximately 0.74, 1.04, 1.13, 1.49, 2.27, 2.53, 2.97, 3.30, 4.80 and 5.27 Hz.

Fig. 4 indicates that the MPC system can decrease the amplitudes for the f_1 -, f_2 -, f_4 - and f_6 -frequencies, for the 3P-frequency as well as for the frequencies at 1.13, 2.27 and 2.97, 3.30 Hz.

The amplitude corresponding to the 1st tower natural frequency (f_1) can be reduced by approximately 80%. The decrease can be attributed the use of the tower top acceleration as controlled variable in the MPC cost function. The MPC predicts the dynamic behavior of the fore-aft movement in order to reduce the arising tower top acceleration. Since the prediction model explicitly includes the 1st natural frequencies of the tower and the blades (flapwise), the MPC can specifically reduce the oscillation amplitudes of the tower as well as the blades corresponding to these frequencies (f_1 , f_2). The prediction model also includes the drivetrain dynamics and thus can specifically reduce the oscillation

amplitude corresponding to the 1st drivetrain natural frequency (f_6).

The prediction model does not consider dynamics with the 3P-frequency. However, the decrease of the amplitudes corresponding to the 3P-frequency could be explained by the use of the tower top acceleration \ddot{x}_t as controlled variable in the MPC system (the BC does not control \ddot{x}_t). Furthermore, the 3P-frequency is close to the f_1 -frequency, which is actively damped by the MPC system (no tower damping is active for the BC).

The experimental results strengthen our simulative analysis in [4], which showed similar results for the occurring mechanical loads in the fore-aft dynamics of the tower compared to the BC system.

The measured tower top acceleration—as kinetic quantity—can only be used to indicate the dynamic mechanical loads in the tower. For a detailed analysis of the mechanical loads, comprehensive simulation studies (as in [4]) or field tests with additional sensors (e.g. with strain gauges) have to be conducted.

Rotational speeds Incremental encoders measure the rotor and generator speeds. These rotational speeds indicate occurring dynamic mechanical loads in the drivetrain.

Fig. 5 and Fig. 6 show FFT plots for the measured generator speed and the deviation of the rotor and generator speed of the experimental field test data of both the BC and the MPC system. In particular, the deviation of the rotational speeds represents the mechanical load situation of the WT's drivetrain. In the both control systems, the generator speed is a controlled variable. The BC provides active drivetrain damping.

The FFT amplitudes in Fig. 5 indicate gain amplifications for both control systems at the f_1 -frequency as well as at the 1P- and 3P-frequencies. Further gain amplifications

Fig. 5 FFT of the measured generator speed of the experimental field test data. Same data basis for the FFT and same markers for the natural frequencies as noted in caption of Fig. 4

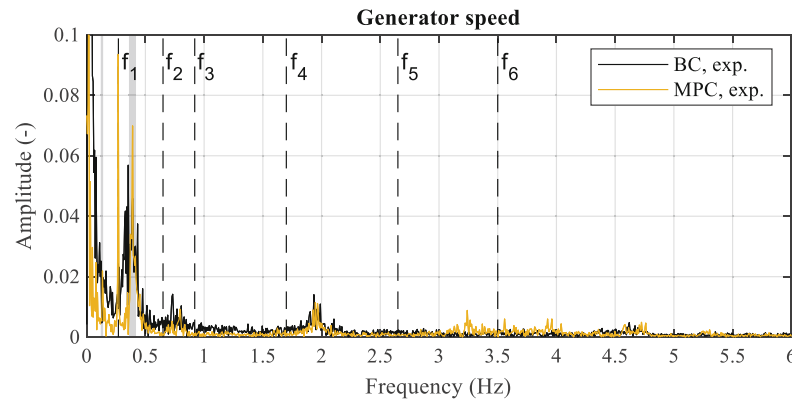
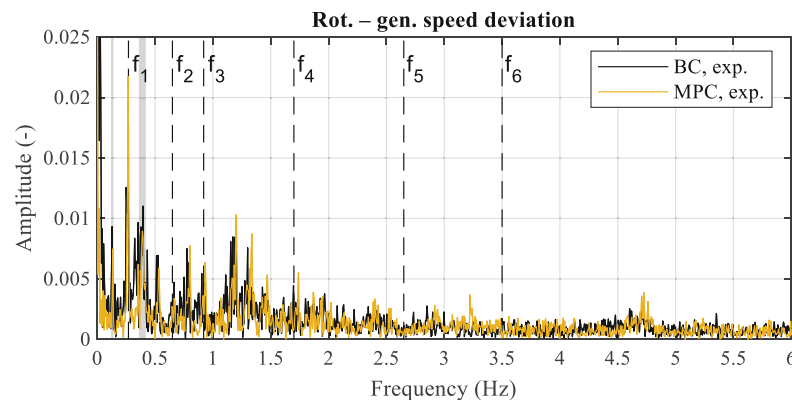


Fig. 6 FFT of the measured deviation between rotor and generator speed of the experimental field test data. Same data basis for the FFT and same markers for the natural frequencies as noted in caption of Fig. 4



can be found again at frequencies of approximately 0.75, 1.95, 3.25, 3.95 and 4.65 Hz.

Fig. 5 indicates reduced amplitudes in the frequency ranges between the 1P-, f_1 - and 3P-frequencies by the MPC system. However, the MPC system increases the amplitudes corresponding to the f_1 - and 3P-frequencies compared to the BC. Moreover, the MPC system can reduce the amplitudes corresponding to the 0.75 Hz-frequency. However, the MPC system increases the amplitudes corresponding to the frequencies at 3.25 and 3.95 Hz.

In Fig. 5, the decrease of the FFT amplitudes in the frequency range between the 1P- and the 3P-frequency can be explained by using the generator speed as controlled variable. The experimental MPC results indicate smaller tracking errors in the deviation between the generator speed and its reference value (not explicitly shown in the previous figures, but indicated in Fig. 3b by smaller values of the interquartile ranges of the generated power for the MPC results compared to the BC results). The reduced tracking error may lead to the observed decrease of the FFT amplitudes.

The increase of the FFT amplitudes at the 1P-, f_1 - and 3P-frequencies can be explained by the MPC command value for the generator torque. The MPC reacts to the oscillations with the occurring frequencies, calculates an appropriate command value for the manipulated variables—particularly

for the generator torque—and applies the generator torque to the drivetrain. Due to the reaction of the MPC system to the occurring frequencies, the 1P-, f_1 - and 3P-frequencies have also an impact on the drivetrain dynamics.

Furthermore, the decrease of the amplitudes corresponding to the 0.75 Hz-frequency indicate a damping of the dynamics corresponding to the 1st (flapwise) blade natural frequency (f_2). Even if the 0.75 Hz-frequency does not exactly match the f_2 -frequency, we attribute the effect to an active f_2 -frequency damping by the MPC system, since the f_2 -frequency correspond to the blade natural frequency for an isolated clamped blade. The corresponding frequency in the overall WT might slightly differ from the “isolated” natural frequency. The gain amplifications in Fig. 5 at the frequencies of 3.25 and 3.95 Hz have to be further analyzed with the simulation models in system simulations and SiL tests in order to investigate the reasons for the increased amplitudes.

Fig. 6 indicates gain amplifications for both control systems at the 1P-, f_1 - and 3P-frequencies. Further gain amplifications can be found at frequencies of approximately 0.75, 1.20, 1.30, 1.45, 1.95, 2.50, 2.90, 3.25 and 4.65 Hz.

As in Fig. 5, Fig. 6 also indicates reduced amplitudes in the frequency ranges between the 1P-, f_1 - and 3P-frequencies by the MPC system as well as increased amplitudes

corresponding to the f_1 -frequency compared to the BC (in Fig. 6, no increase can be found for the 3P-frequency).

Again, the MPC system can reduce the amplitudes that correspond to frequencies between the f_2 - and 0.75 Hz-frequencies. As before, we assume the active f_2 -frequency damping by the MPC system to be responsible for the reduced amplitudes.

The MPC system increases the amplitudes corresponding to the frequencies at 3.25 and 4.65 Hz; these gain amplifications have to be further analyzed with the simulation models in system simulations and SiL tests.

On this basis, the load situation in the drivetrain indicates reduced amplitudes for certain frequencies considered in the prediction model of the MPC. In particular, the FFT plot of the deviation between the rotational speeds (Fig. 6) indicates similar amplitudes for the BC and the MPC system (with the exceptions mentioned above).

Hence, the experimental field test results correspond to our findings in prior simulation studies [4], which indicate a similar mechanical load situation for the MPC system and the BC, respectively.

3.4 Analysis of the PLC's computing and communication times

During the field test, the DUT-PLC executes the MPC system (compare Fig. 1).

Fig. 7 shows the distribution of the computing time of the MPC system (MPC algorithm and extended Kalman filter) in the DUT-PLC (with a PLC cycle time of 100 ms) during the field test. Fig. 7 indicates mean and maximum computing times of 16.9 ms and 21.4 ms, respectively, and a standard deviation of 0.3 ms. Consequently, the MPC system requires approximately 17–21% of the cycle time of the DUT-PLC and is real-time capable without overloading the PLC. The experimental field test results of the PLC's computing times correspond to our findings in prior HiL tests [3] (which showed mean and maximal values of 16.9 ms and 20.8 ms, respectively).

The communication time of the hardware setup according to Fig. 1a results in a communication delay time of approximately 90 ms. According to the HiL tests, we expected a communication delay time of approximately 2–4 PLC cycle times (20–40 ms). Since communication delay times of 20–40 ms had no significant effects on the simulative MPC results in SiL and HiL tests, we did not consider any delay times in the current MPC formulation.

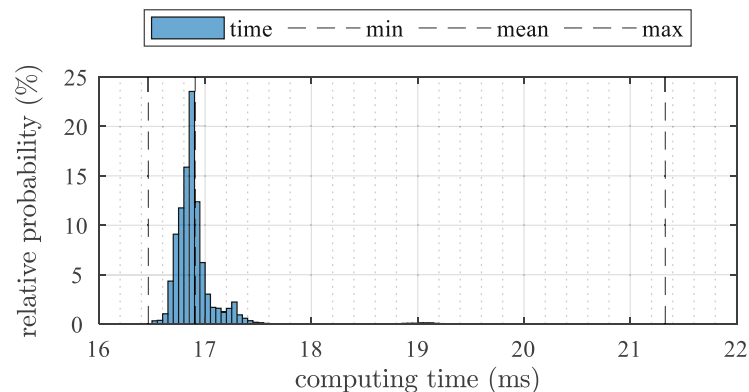
4 Conclusion and outlook

In this study, we successfully established the functional and structural integration of the real-time linear time-variant MPC with weight-scheduling, introduced in detail in our companion paper [4], into the automation system of the WT “W2E-120/3.0fc”.

The MPC system was in full control of the 3 MW WT for an overall operating time of approximately 90 min. To the authors' best knowledge, for the first time in the academic field of MPC for WTs, this study provides experimental MPC results from a full-scale field test in a multi-megawatt WT.

The MPC system offers similar experimental results for the electrical power output and the occurring mechanical loads compared to the BC in the partial load region between wind speeds of approximately 5.0–7.5 m/s. The experimental results indicate a slight average reduction of the interquartile ranges of the power output from 63 to 48 kW (approx. 25% reduction) by using the MPC system. Thus, the MPC system reduces the power fluctuations while maintaining the median values of the power output on a similar level in the tested partial load region. For the tower top acceleration, the oscillation amplitudes corresponding to the 1st tower and the 1st (flapwise) blade natural frequency can be significantly reduced by the MPC system; the gain amplification corresponding to the 1st tower natural frequency can be reduced by approximately 80%. Moreover, the MPC computing times verify real-time capability of the MPC system in the DUT-PLC (mean and maximum computing

Fig. 7 Computing time of the MPC system in DUT-PLC (Bachmann's MH230 PLC) during the field test (standard deviation 0.3 ms, PLC cycle time 100 ms)



times of 16.9 ms and 21.4 ms, respectively, with a PLC cycle time of 100 ms). The experimental results correspond to our findings in prior simulative SiL tests [4] and HiL tests [3] and encourage a systematic MPC development in a simulative environment with SiL and HiL tests.

Thus, with the field test, we could validate the rapid control prototyping process as well as the test environment for systematic MPC development introduced in [3]. We exclusively tuned the MPC parameters in the proposed simulative environment. Since we could fully validate the functional as well as the structural integration of the MPC system in SiL and HiL tests prior to the field test, we were able to realize the MPC commissioning in the DUT-PLC within a few hours without any modifications—neither to the software nor to the hardware. Thus, the field test verifies the capability of the proposed rapid control prototyping process to minimize the application effort and the time required for the MPC commissioning in the WT automation system. To the author's best knowledge, for the first time in the academic field of MPC for WTs, a systematic development process has been validated in a full-scale field test.

With this study, we could bridge the existing gap between the control design and field testing of MPC systems for WTs in the multi-megawatt range. As a result, we successfully established a continuous toolchain between the simulative development environment and the WT's automation system, which is available for further field tests of MPC systems in the real WT.

For future studies, we are going to adapt the MPC algorithm and modify the SiL and HiL test stages according to the findings of the experimental field test results. In particular, we are going to investigate the natural frequency at approximately 4.65 Hz with the WT plant model in the simulation environment and—depending on the simulative results—we will additionally consider this frequency in the prediction model of the MPC algorithm.

The occurring communication delay time of 90 ms should be further emulated in the HiL setup and could be considered in future MPC implementations. SiL and HiL tests can help to evaluate the impact of such communication delay times.

Since in the field test, only measurements in the partial load region could be captured, further tests would be necessary to investigate the MPC performance in the full load region in order to validate the potential of the MPC system in the real WT over the entire operating range.

Acknowledgements We would like to thank all colleagues from *W2E Wind to Energy* involved in the MPC test campaign for all the help in the organization as well as for all the support in commissioning the MPC system in the real wind turbine and in conducting the field test. Moreover, the authors thank *Bachmann electronic* for their technical support and for providing an MH230 PLC module for preparing and conducting the field test.

Funding Open Access funding enabled and organized by Projekt DEAL.

Open Access This article is licensed under a Creative Commons Attribution 4.0 International License, which permits use, sharing, adaptation, distribution and reproduction in any medium or format, as long as you give appropriate credit to the original author(s) and the source, provide a link to the Creative Commons licence, and indicate if changes were made. The images or other third party material in this article are included in the article's Creative Commons licence, unless indicated otherwise in a credit line to the material. If material is not included in the article's Creative Commons licence and your intended use is not permitted by statutory regulation or exceeds the permitted use, you will need to obtain permission directly from the copyright holder. To view a copy of this licence, visit <http://creativecommons.org/licenses/by/4.0/>.

References

- van Kuik GAM, Peinke J, Nijssen R, Lekou D, Mann J, Sørensen JN, Ferreira C, van Wingerden JW, Schlipf D, Gebraad P, Polinder H, Abrahamsen A, van Bussel GJW, Sørensen JD, Tavner P, Bottasso CL, Muskulus M, Matha D, Lindeboom HJ, Degraer S, Kramer O, Lehnhoff S, Sonnenschein M, Sørensen PE, Küneke RW, Morthorst PE, Skytte K (2016) Long-term research challenges in wind energy—a research agenda by the European Academy of Wind Energy. *Wind Energy Sci*. <https://doi.org/10.5194/wes-1-1-2016>
- Schulze A, Zierath J, Rosenow S-E, Bockhahn R, Rachholz R, Wernle C (2018) Passive structural control techniques for a 3 MW wind turbine prototype. *J Phys Conf Ser*. <https://doi.org/10.1088/1742-6596/1037/4/042024>
- Dickler S, Kallen T, Zierath J, Abel D (2020) Rapid control prototyping of model predictive wind turbine control toward field testing. *J Phys Conf Ser*. <https://doi.org/10.1088/1742-6596/1618/2/022068>
- Wintermeyer-Kallen T, Dickler S, Zierath J, Konrad T, Abel D (2021) Weight-scheduling for linear time-variant model predictive wind turbine control toward field testing. In: 2021 Conference for Wind Power Drives (CWD) Aachen, Germany (accepted)
- Lio WH, Rossiter JA, Jones BL (2014) A review on applications of model predictive control to wind turbines. In: 2014 UKACC International Conference on Control (CONTROL). IEEE, Loughborough, pp 673–678 <https://doi.org/10.1109/CONTROL.2014.6915220>
- Gros S, Schild A (2017) Real-time economic nonlinear model predictive control for wind turbine control. *Int J Control*. <https://doi.org/10.1080/00207179.2016.1266514>
- Guadayol Roig M (2017) Application of model predictive control to wind turbines. Dissertation, ETH Zurich. <https://doi.org/10.3929/ethz-b-000218664>
- Castaing D, Barlas T, Buhl T, Poulsen NK, Wedel-Heinen JJ, Olesen NA, Bak C, Kim T (2014) Full-scale test of trailing edge flaps on a Vestas V27 wind turbine: active load reduction and system identification. *Wind Energy*. <https://doi.org/10.1002/we.1589>
- Bottasso CL, Pizzinelli P, Riboldi CED, Tasca L (2014) LiDAR-enabled model predictive control of wind turbines with real-time capabilities. *Renew Energy*. <https://doi.org/10.1016/j.renene.2014.05.041>
- Verwaal NW, van der Veen GJ, van Wingerden JW (2015) Predictive control of an experimental wind turbine using preview wind speed measurements. *Wind Energy*. <https://doi.org/10.1002/we.1702>
- Vukov M, Gros S, Horn G, Frison G, Geebelen K, Jørgensen JB, Swevers J, Diehl M (2015) Real-time nonlinear MPC and MHE for

- a large-scale mechatronic application. *Control Eng Pract.* <https://doi.org/10.1016/j.conengprac.2015.08.012>
12. Zierath J, Jassmann U, Dickler S, Abel D (2016) Testing model predictive control algorithms for wind turbine control by means of a hardware-in-the-loop test rig. In: 4th Joint International Conference on Multibody System Dynamics (IMSD) Montreal, Canada
 13. Jassmann U, Zierath J, Dickler S, Abel D (2016) Model predictive wind turbine control for load alleviation and power leveling in extreme operation conditions. In: IEEE Conference on Control Applications (CCA) Buenos Aires, Argentina, pp 1368–1373 <https://doi.org/10.1109/CCA.2016.7587997>
 14. Ferreau HJ, Kirches C, Potschka A, Bock HG, Diehl M (2014) qpOASES: a parametric active-set algorithm for quadratic programming. *Math Program Comput.* <https://doi.org/10.1007/s12532-014-0071-1>
 15. Zierath J, Jassmann U, Abel D (2015) Capabilities of model predictive control for load reduction on wind turbines. In: Proceedings of the ECCOMAS Thematic Conference on Multibody Dynamics 2015 Barcelona, Spain, pp 776–788